

Constraints on primordial black holes from N_{eff} : scalar induced gravitational waves as an extra radiation component

JING-ZHI ZHOU,¹ YU-TING KUANG,^{2,3} ZHE CHANG,^{2,3} AND H. LÜ^{1,4}

¹Center for Joint Quantum Studies and Department of Physics, School of Science, Tianjin University, Tianjin 300350, China

²Institute of High Energy Physics, Chinese Academy of Sciences, Beijing 100049, China

³University of Chinese Academy of Sciences, Beijing 100049, China

⁴Joint School of National University of Singapore and Tianjin University, International Campus of Tianjin University, Binhai New City, Fuzhou 350207, China

ABSTRACT

In June 2023, multiple pulsar timing array collaborations provided evidence for the existence of a stochastic gravitational wave background. Scalar induced gravitational waves (SIGWs), as one of the most likely sources of stochastic gravitational waves, have received widespread attention. When primordial curvature perturbations on small scales are sufficiently large, primordial black holes (PBHs) inevitably form, concurrently producing SIGWs with significant observable effects. These SIGWs can serve as an additional radiation component, influencing the relativistic degrees of freedom N_{eff} . Taking into account primordial non-Gaussianity, we study the energy density spectrum of SIGWs up to the third order and use the current observational data of N_{eff} to constrain small-scale primordial curvature perturbations and the abundance of PBHs.

Keywords: Primordial black hole — Scalar induced gravitational wave — Primordial curvature perturbation — Primordial non-Gaussianity

1. INTRODUCTION

Current cosmological observations suggest the existence of dark matter in our universe. As one of the significant candidates for dark matter, PBHs have garnered extensive attention over the past decade. PBHs originate from primordial curvature perturbations with large amplitudes on small scales Bird et al. (2016); García-Bellido (2017); Barack et al. (2019); Byrnes et al. (2019); Chen et al. (2024). Specifically, on large scales ($\gtrsim 1$ Mpc), cosmological observations like the cosmic microwave backgrounds (CMB) and large scale structures (LSS) have tightly constrained the amplitude of the primordial curvature perturbation power spectrum to $A_\zeta \sim 2 \times 10^{-9}$ Aghanim et al. (2020); Abdalla et al. (2022). The tensor-to-scalar ratio r on large scales is restricted to below 0.06. However, on small scales ($\lesssim 1$ Mpc), there are no particularly stringent experimental observational constraints on primordial curvature perturbations Bringmann et al. (2012). This enables large amplitude primordial perturbations on small scales to

re-enter the horizon after inflation, resulting in significant density perturbations and the formation of PBHs Sasaki et al. (2018); Carr et al. (2021).

The process during which the PBHs are formed would be inevitably accompanied by the generation of SIGWs Matarrese et al. (1998); Mollerach et al. (2004); Ananda et al. (2007); Baumann et al. (2007); Saito & Yokoyama (2009); Bugaev & Klimai (2010, 2011); Yuan et al. (2019); Papanikolaou et al. (2021); Chang et al. (2023); Choudhury et al. (2024); Domènec & Tränkle (2024). In June 2023, multiple international PTA collaborations, including NANOGrav Agazie et al. (2023), PPTA Reardon et al. (2023), EPTA Antoniadis et al. (2023), and CPTA Xu et al. (2023), presented evidence supporting the existence of a stochastic gravitational wave background (SGWBs) in the nHz frequency range. SIGWs, as one of the most likely sources of the stochastic gravitational wave background, have garnered significant attention Franciolini et al. (2023); Ellis et al. (2024); Domènec et al. (2024); Hosseini Mansoori et al. (2023); Harigaya et al. (2023). Utilizing current pulsar timing array (PTA) data, we can investigate the impact of SIGWs on current SGWBs, thereby constraining the

parameter space of the primordial power spectrum on small scales and the abundance of PBHs. Furthermore, current PTA data can be used to investigate potential new physics that might have existed during the evolution of the universe Yu & Wang (2024); Sui et al. (2024); Zhou et al. (2024a); Papanikolaou et al. (2024); Papanikolaou (2023).

In this paper, we consider the impact of SIGWs with primordial non-Gaussianity as an additional radiation component on cosmological evolution. More precisely, current large-scale cosmological observations, such as CMB, LSS, and baryon acoustic oscillations (BAO) provide stringent constraints on the relativistic degrees of freedom parameter N_{eff} Jiang et al. (2024); Ben-Dayan et al. (2019); Clarke et al. (2020); Cang et al. (2023); Wang et al. (2024). When we consider the additional contribution of SIGWs to the radiation components, this additional radiation component will inevitably affect the parameter N_{eff} , and this effect must not exceed the bounds on N_{eff} determined by current large-scale cosmological observations. Utilizing the current observational data of N_{eff} , we can constrain the energy density spectrum of SIGWs, thereby limiting and excluding the parameter space of the primordial power spectrum on small scales. Since the primordial power spectrum directly influences the calculation of the abundance of PBHs, this physical process can also be used to constrain the abundance of PBHs of different masses.

This paper is organized as follows. In Sec. 2, we review the calculations of second and third order SIGWs. In Sec. 3, we calculate the energy density spectrum of SIGWs up to third order. In Sec. 4, we discuss the constraints on the abundance of PBHs from large-scale cosmological observations. Finally, we summarize our results and give some discussions in Sec. 5.

2. SECOND AND THIRD ORDER SIGWS

Due to the potential presence of significant primordial curvature perturbations on small scales, higher-order SIGWs can have a substantial impact on the total energy density spectrum of SIGWs. Ignoring the higher-order contributions of SIGWs will lead to severe deviations in the predicted energy density spectrum of SIGWs. Therefore, it is crucial to consider the impact of higher-order effects on the energy density spectrum of SIGWs. In this section, we briefly review the main results of second order and third order SIGWs. The perturbed metric in the Friedmann-Lemaitre-Robertson-Walker (FLRW)

spacetime with Newtonian gauge takes the form

$$ds^2 = a^2 \left(- \left(1 + 2\phi^{(1)} + \phi^{(2)} \right) d\eta^2 + V_i^{(2)} d\eta dx^i + \left(\left(1 - 2\psi^{(1)} - \psi^{(2)} \right) \delta_{ij} + \frac{1}{2} h_{ij}^{(2)} + \frac{1}{6} h_{ij}^{(3)} \right) dx^i dx^j \right), \quad (1)$$

where $h_{ij}^{(n)}$ ($n = 2, 3$) are second order and third order tensor perturbations. $\phi^{(n)}$ and $\psi^{(n)}$ ($n = 1, 2$) are first order and second order scalar perturbations. $V_i^{(2)}$ is second order vector perturbation. By substituting the metric perturbations in Eq. (1) into the Einstein field equation and simplifying, we can derive the equations of motion of the cosmological perturbations at each order Zhou et al. (2024b). To obtain the explicit expressions for the second order and third order SIGWs, we need to start with the first order scalar perturbations and solve these cosmological perturbation equations order by order. After solving the first order scalar perturbations, we can derive the specific expression for the second order SIGWs Kohri & Terada (2018)

$$h_{\mathbf{k}}^{\lambda, (2)}(\eta) = \frac{4}{9} \int \frac{d^3 p}{(2\pi)^{3/2}} \varepsilon^{\lambda, lm}(\mathbf{k}) p_l p_m \zeta_{\mathbf{k}-\mathbf{p}} \zeta_{\mathbf{p}} I^{(2)}(u, v), \quad (2)$$

where

$$I^{(2)}(u, v) = \frac{27}{64} \left(\frac{3(u^2 + v^2 - 3) \left(-4v^2 + (1 - u^2 + v^2)^2 \right)}{16u^4 v^4} \right)^2 \left(\left(-4uv + (u^2 + v^2 - 3) \log \left| \frac{3 - (u+v)^2}{3 - (u-v)^2} \right| \right)^2 + \pi^2 (u^2 + v^2 - 3)^2 \Theta(u + v - \sqrt{3}) \right) \quad (3)$$

is known as the kernel function of second order SIGWs. Here, we have defined $|\mathbf{k} - \mathbf{p}| = u|\mathbf{k}|$ and $|\mathbf{p}| = v|\mathbf{k}|$.

For third order SIGWs, first order scalar perturbations directly induce three types of second order perturbations. These three second order perturbations, together with the first order scalar perturbations, subsequently induce third order SIGWs Chang et al. (2024a); Zhou et al. (2022). The specific expression for the third order SIGWs can be represented as

$$h_{\mathbf{k}}^{\lambda, (3)}(\eta) = h_{\mathbf{k}, \phi\phi\phi}^{\lambda, (3)}(\eta) + h_{\mathbf{k}, \phi h_{\phi\phi}}^{\lambda, (3)}(\eta) + h_{\mathbf{k}, \phi V_{\phi\phi}}^{\lambda, (3)}(\eta) + h_{\mathbf{k}, \phi\psi_{\phi\phi}}^{\lambda, (3)}(\eta), \quad (4)$$

where

$$h_{\mathbf{k}, \phi\phi\phi}^{\lambda, (3)}(\eta) = \int \frac{d^3 p}{(2\pi)^{3/2}} \int \frac{d^3 q}{(2\pi)^{3/2}} \varepsilon^{\lambda, lm}(\mathbf{k}) q_m \times (p_l - q_l) \frac{8}{27} I_{\phi\phi\phi}^{(3)}(u, \bar{u}, \bar{v}, x) \zeta_{\mathbf{k}-\mathbf{p}} \zeta_{\mathbf{p}-\mathbf{q}} \zeta_{\mathbf{q}}, \quad (5)$$

$$h_{\mathbf{k}, \phi h_{\phi\phi}}^{\lambda, (3)}(\eta) = \int \frac{d^3 p}{(2\pi)^{3/2}} \int \frac{d^3 q}{(2\pi)^{3/2}} \varepsilon^{\lambda, lm}(\mathbf{k}) \Lambda_{lm}^{rs}(\mathbf{p}) \\ \times q_r q_s \frac{8}{27} I_{\phi h_{\phi\phi}}^{(3)}(u, \bar{u}, \bar{v}, x) \zeta_{\mathbf{k}-\mathbf{p}} \zeta_{\mathbf{p}-\mathbf{q}} \zeta_{\mathbf{q}}, \quad (6)$$

$$h_{\mathbf{k}, \phi V_{\phi\phi}}^{\lambda, (3)}(\eta) = \int \frac{d^3 p}{(2\pi)^{3/2}} \int \frac{d^3 q}{(2\pi)^{3/2}} \varepsilon^{\lambda, lm}(\mathbf{k}) \mathcal{T}_{(m)}^r(\mathbf{p}) p_l \\ \times \frac{16 p^s}{27 p^2} q_r q_s I_{\phi V_{\phi\phi}}^{(3)}(u, \bar{u}, \bar{v}, x) \zeta_{\mathbf{k}-\mathbf{p}} \zeta_{\mathbf{p}-\mathbf{q}} \zeta_{\mathbf{q}}, \quad (7)$$

$$h_{\mathbf{k}, \phi \psi_{\phi\phi}}^{\lambda, (3)}(\eta) = \int \frac{d^3 p}{(2\pi)^{3/2}} \int \frac{d^3 q}{(2\pi)^{3/2}} \varepsilon^{\lambda, lm}(\mathbf{k}) p_l p_m \\ \times \frac{8}{27} I_{\phi \psi_{\phi\phi}}^{(3)}(u, \bar{u}, \bar{v}, x) \zeta_{\mathbf{k}-\mathbf{p}} \zeta_{\mathbf{p}-\mathbf{q}} \zeta_{\mathbf{q}}. \quad (8)$$

Here, we have defined $x = |\mathbf{k}| \eta$. In Eq. (5), we use the symbol $h_{\mathbf{k}, \phi\phi\phi}^{(3)}$ to represent the third order SIGWs sourced by three first order scalar perturbations Chen et al. (2023). Eq. (6)–Eq. (8) represent third order SIGWs induced by three types of second order perturbations together with first order scalar perturbations. The explicit expressions of the third order kernel functions $I^{(3)}$ can be found in Ref. Zhou et al. (2022).

3. ENERGY DENSITY OF SIGWS

In this section, we utilize the specific expressions for second order and third order SIGWs provided in the previous section to study the energy density spectra of SIGWs. The energy density spectrum of SIGWs is defined as

$$\overline{\Omega}_{\text{GW}}(\eta, k) = \overline{\rho_{\text{GW}}(\eta, k)} = \frac{x^2}{6} \mathcal{P}_h(\eta, k), \quad (9)$$

where

$$\mathcal{P}_h(\eta, k) = \frac{1}{4} \mathcal{P}_h^{(2,2)}(\eta, k) + \frac{1}{6} \mathcal{P}_h^{(2,3)}(\eta, k) + \frac{1}{36} \mathcal{P}_h^{(3,3)}(\eta, k) \\ + O(\mathcal{P}_h^{(4,n)}) \quad (10)$$

is the total power spectrum of SIGWs. The overline represents the oscillation average. The power spectrum $\mathcal{P}_k^{(m,n)}(\eta)$ can be calculated in terms of the two-point correlation function of $h_{\mathbf{k}}^{\lambda, (m)}(\eta)$ and $h_{\mathbf{k}'}^{\lambda, (n)}(\eta)$

$$\langle h_{\mathbf{k}}^{\lambda, (m)}(\eta) h_{\mathbf{k}'}^{\lambda', (n)}(\eta) \rangle = \delta^{\lambda\lambda'} \delta(\mathbf{k} + \mathbf{k}') \frac{2\pi^2}{k^3} \mathcal{P}_k^{(m,n)}(\eta). \quad (11)$$

Before calculating the total energy density spectrum of SIGWs, we can first analyze the structure of the two-point correlation function $\langle h_{\mathbf{k}}^{\lambda, (m)}(\eta) h_{\mathbf{k}'}^{\lambda', (n)}(\eta) \rangle$. Specifically, as shown in Eq. (4)–Eq. (8) and Eq. (2), the second order SIGW is proportional to two primordial curvature perturbations: $h_{\mathbf{k}}^{\lambda, (2)}(\eta) \sim \zeta_{\mathbf{k}-\mathbf{p}} \zeta_{\mathbf{p}}$, and the third

order SIGW is proportional to three primordial curvature perturbations: $h_{\mathbf{k}}^{\lambda, (3)}(\eta) \sim \zeta_{\mathbf{k}-\mathbf{p}} \zeta_{\mathbf{p}-\mathbf{q}} \zeta_{\mathbf{q}}$. When we only consider Gaussian-type primordial curvature perturbations, the n -point correlation function of the primordial curvature perturbations is strictly zero when n is odd. Therefore, the two-point correlation function $\langle h_{\mathbf{k}}^{\lambda, (m)}(\eta) h_{\mathbf{k}'}^{\lambda', (n)}(\eta) \rangle$ only has non-zero results when $n = m = 2$ and $n = m = 3$, namely

$$\langle h_{\mathbf{k}}^{\lambda, (2)}(\eta) h_{\mathbf{k}'}^{\lambda', (2)}(\eta) \rangle \sim \langle \zeta_{\mathbf{k}-\mathbf{p}} \zeta_{\mathbf{p}} \zeta_{\mathbf{k}'-\mathbf{p}'} \zeta_{\mathbf{p}'} \rangle \\ \sim \mathcal{P}_\zeta \mathcal{P}_\zeta \sim A_\zeta^2, \quad (12)$$

$$\langle h_{\mathbf{k}}^{\lambda, (3)}(\eta) h_{\mathbf{k}'}^{\lambda', (3)}(\eta) \rangle \sim \langle \zeta_{\mathbf{k}-\mathbf{p}} \zeta_{\mathbf{p}-\mathbf{q}} \zeta_{\mathbf{q}} \zeta_{\mathbf{k}'-\mathbf{p}'} \zeta_{\mathbf{p}'-\mathbf{q}'} \zeta_{\mathbf{q}'} \rangle \\ \sim \mathcal{P}_\zeta \mathcal{P}_\zeta \mathcal{P}_\zeta \sim A_\zeta^3, \quad (13)$$

where \mathcal{P}_ζ is the power spectrum of primordial curvature perturbation which is defined as $\langle \zeta_{\mathbf{k}} \zeta_{\mathbf{k}'} \rangle = \frac{2\pi^2}{k^3} \delta(\mathbf{k} + \mathbf{k}') \mathcal{P}_\zeta(k)$. A_ζ is the amplitude of the primordial power spectrum.

In this paper, we consider the local type non-Gaussianity which can be expressed as a local perturbative expansion around the Gaussian primordial curvature perturbation. The primordial curvature perturbation in momentum space can be rewritten as Cai et al. (2019); Adshead et al. (2021); Domènech (2021); Chang et al. (2024b)

$$\zeta_{\mathbf{k}}^{\text{ng}} = \zeta_{\mathbf{k}} + \frac{3}{5} f_{\text{NL}} \int \frac{d^3 \mathbf{n}}{(2\pi)^{3/2}} \zeta_{\mathbf{k}-\mathbf{n}} \zeta_{\mathbf{n}}. \quad (14)$$

Here, we consider the lowest-order contribution of the non-Gaussian parameter f_{NL} . In this case, the contribution of the two point correlation function $\langle h_{\mathbf{k}}^{\lambda, (m)}(\eta) h_{\mathbf{k}'}^{\lambda', (n)}(\eta) \rangle$ to the total power spectrum $\mathcal{P}_h(\eta, k)$ of SIGWs can be divided into four parts

$$\langle h_{\mathbf{k}}^{\lambda, (2)}(\eta) h_{\mathbf{k}'}^{\lambda', (2)}(\eta) \rangle \sim A_\zeta^2, \quad \langle h_{\mathbf{k}}^{\lambda, (3)}(\eta) h_{\mathbf{k}'}^{\lambda', (3)}(\eta) \rangle \sim A_\zeta^3, \\ \langle h_{\mathbf{k}}^{\lambda, (3)}(\eta) h_{\mathbf{k}'}^{\lambda', (2)}(\eta) \rangle \sim f_{\text{NL}} A_\zeta^3, \\ \langle h_{\mathbf{k}}^{\lambda, (2)}(\eta) h_{\mathbf{k}'}^{\lambda', (2)}(\eta) \rangle \sim (f_{\text{NL}})^2 A_\zeta^3. \quad (15)$$

By substituting Eq. (4)–Eq. (8) and Eq. (2) into Eq. (11), we can derive the expression for the total power spectrum $\mathcal{P}_h(\eta, k)$ of SIGWs. Subsequently, using Eq. (9), we can calculate the total energy density spectrum of SIGWs. Taking into account the thermal history of the universe, we obtain the current total energy density spectrum of SIGWs $\Omega_{\text{GW},0}$ Wang et al. (2019)

$$\Omega_{\text{GW},0}(k) = \Omega_{\text{rad},0} \left(\frac{g_{*,\rho,e}}{g_{*,\rho,0}} \right) \left(\frac{g_{*,s,0}}{g_{*,s,e}} \right)^{4/3} \overline{\Omega}_{\text{GW}}(\eta, k), \quad (16)$$

where $\Omega_{\text{rad},0} \approx 4.2 \times 10^{-5}/h^2$ is the physical energy density fraction of radiations in the present universe.

The effect numbers of relativistic species $g_{*,\rho}$ and $g_{*,s}$ can be found in Ref. Saikawa & Shirai (2018). And $h = 0.6766$ is the dimensionless Hubble constant. By integrating the energy density spectrum of SIGWs, we obtain the energy density of SIGWs

$$\rho_{\text{GW}}/\rho_{\text{tot},0} = \int_0^\infty \Omega_{\text{GW},0}(k) d(\ln k) . \quad (17)$$

Given the power spectrum of primordial curvature perturbations, we can calculate the energy density spectrum of SIGWs and the corresponding energy density. Here, we consider the log-normal primordial power spectrum

$$\mathcal{P}_\zeta(k) = \frac{A_\zeta}{\sqrt{2\pi}\sigma^2} \exp\left(-\frac{\ln^2(k/k_*)}{2\sigma^2}\right) , \quad (18)$$

where A_ζ is the amplitude of primordial power spectrum and $k_* = 2\pi f_*$ is the wavenumber at which the primordial power spectrum has a log-normal peak. We calculate the total energy density $\rho_{\text{GW}}/\rho_{\text{tot},0}$ of SIGWs for different A_ζ and f_{NL} . As shown in Fig. 1, the green and orange lines represent the total energy density of SIGWs for non-Gaussian parameters $f_{\text{NL}} = 5$ and $f_{\text{NL}} = -5$, respectively. It shows that the energy density for $f_{\text{NL}} = -5$ is significantly lower than that for $f_{\text{NL}} = 5$. The presence of the cross two-point correlation function $\langle h_{\mathbf{k}}^{\lambda,(3)} h_{\mathbf{k}'}^{\lambda',(2)} \rangle \sim f_{\text{NL}} A_\zeta^3$ causes a significant decrease in the total energy density spectrum of SIGWs when the non-Gaussian parameter f_{NL} is negative. When f_{NL} is sufficiently large, the contribution of the two-point correlation function $\langle h_{\mathbf{k}}^{\lambda,(2)} h_{\mathbf{k}'}^{\lambda',(2)} \rangle \sim (f_{\text{NL}})^2 A_\zeta^3$ becomes dominant, and the suppressing effect of the cross two-point correlation function $\langle h_{\mathbf{k}}^{\lambda,(3)} h_{\mathbf{k}'}^{\lambda',(2)} \rangle \sim f_{\text{NL}} A_\zeta^3$ on the total energy density becomes negligible Chang et al. (2024b). Additionally, the black dashed line in fig. 1 represents the energy density spectrum with second-order SIGWs considered only. The difference between the black solid line and the black dashed line reveals that third-order SIGWs substantially increase the total energy density of SIGWs.

4. CONSTRAINTS ON PBHs

When the primordial curvature perturbations on small scales are sufficiently large, PBHs will inevitably form. The PBH mass fraction at formation time can be calculated as Young & Byrnes (2013); Byrnes et al. (2012)

$$\beta(M) \approx \frac{1}{2} \begin{cases} \operatorname{erfc}\left(\frac{\zeta_G^+(\zeta_c)}{\sqrt{2\langle\zeta_G^2\rangle}}\right) + \operatorname{erfc}\left(-\frac{\zeta_G^-(\zeta_c)}{\sqrt{2\langle\zeta_G^2\rangle}}\right); \\ \qquad \qquad \qquad f_{\text{NL}} > 0, \\ \operatorname{erf}\left(\frac{\zeta_G^+(\zeta_c)}{\sqrt{2\langle\zeta_G^2\rangle}}\right) - \operatorname{erf}\left(\frac{\zeta_G^-(\zeta_c)}{\sqrt{2\langle\zeta_G^2\rangle}}\right); \\ \qquad \qquad \qquad f_{\text{NL}} < 0, \end{cases} \quad (19)$$

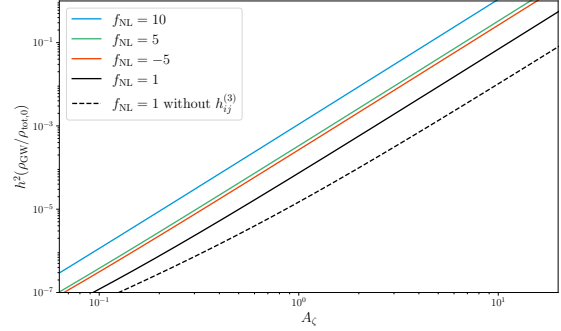


Figure 1. Energy density of SIGWs ($\rho_{\text{GW}}/\rho_{\text{tot},0}$) as a function of A_ζ . Different curves represent varying values of f_{NL} . The black dashed line denotes the energy density when only second-order SIGWs $h_{ij}^{(2)}$ are considered. We have set $\sigma = 0.5$.

where

$$\zeta_G^\pm(\zeta) \approx \frac{5}{6f_{\text{NL}}} \left(-1 \pm \sqrt{1 + \frac{12}{5}f_{\text{NL}}\zeta} \right) . \quad (20)$$

And ζ_c is the threshold value Musco et al. (2009, 2005); Harada et al. (2013). The abundance of PBHs is given by Sasaki et al. (2018)

$$f_{\text{pbh}} \simeq 2.5 \times 10^8 \beta \left(\frac{g_*^{\text{form}}}{10.75} \right)^{-\frac{1}{4}} \left(\frac{m_{\text{pbh}}}{M_\odot} \right)^{-\frac{1}{2}} . \quad (21)$$

Given the primordial power spectrum, we can use Eq. (19) and Eq. (21) to calculate the abundance of PBHs. In the subsequent discussion, we will analyze the constraints that current N_{eff} observational data impose on both the primordial power spectrum and the abundance of PBHs.

After the decoupling of neutrinos, the cosmic radiation energy density ρ_{rad} includes CMB photons γ , neutrinos ν , and the density of SIGWs

$$\rho_{\text{rad}} = \rho_\gamma + \rho_\nu + \rho_{\text{GW}} . \quad (22)$$

The relationship between the three energy densities, CMB temperature, and the relativistic degrees of freedom N_{eff} can be expressed as

$$\rho_\gamma = \frac{\pi^2}{15} T_\gamma^4 , \quad (23)$$

$$\rho_\nu + \rho_{\text{GW}} = \frac{7\pi^2}{120} N_{\text{eff}} T_\nu^4 , \quad (24)$$

where $T_\gamma = 2.728(1+z)$ K and $T_\nu = (4/11)^{1/3}T_\gamma$ K are temperatures of CMB and neutrino respectively. The energy density of SIGWs can affect N_{eff} , and the upper

limit of this effect is constrained by current cosmological observations. In this case, the total energy density spectrum of SIGWs satisfies Ben-Dayan et al. (2019); Clarke et al. (2020); Cang et al. (2023); Wang et al. (2024); Wright et al. (2024)

$$\int_{f_{\min}}^{\infty} h^2 \Omega_{\text{GW},0}(k) d(\ln k) < 1.3 \times 10^{-6} \frac{\Delta N_{\text{eff}}}{0.234}. \quad (25)$$

where $\Delta N_{\text{eff}} = N_{\text{eff}} - 3.046$. We utilize the N_{eff} limits provided by Aghanim et al. (2020), which report $N_{\text{eff}} = 3.04 \pm 0.22$ at a 95% confidence level for the Planck + BAO + BBN data. By applying Gaussian statistics, this translates to a 95% confidence level upper limit of $\Delta N_{\text{eff}} < 0.175$. Using Eq. (25), we can provide the current cosmological constraints on the primordial power spectrum based on observations of N_{eff} . As shown in Fig. 2, we present the current constraints on the small-scale primordial power spectrum based on the Planck + BAO + BBN data Aghanim et al. (2020). In Fig. 2, the three curves represent the rela-

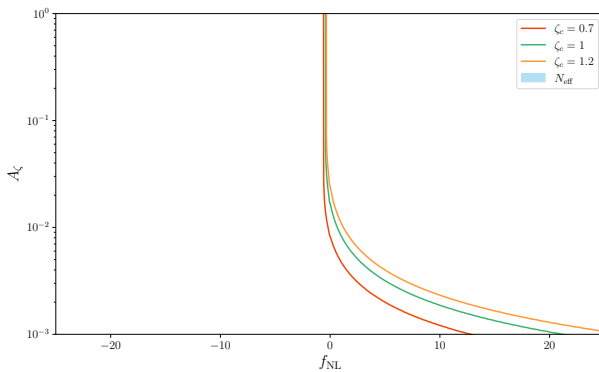


Figure 2. Constraints on A_ζ under different values of f_{NL} . The shaded blue region represents the allowed area constrained by current observations of N_{eff} . The three curves indicate the upper limits of A_ζ for different values of f_{NL} under the condition $f_{\text{pbh}} = 1$ and $m_{\text{pbh}} = 10^{-12} M_\odot$, where M_\odot denotes the solar mass. We have chosen the threshold value ζ_c to be 0.7, 1, and 1.2, respectively.

tionship between parameter A_ζ and f_{NL} when the primordial black hole abundance f_{pbh} is set to 1. It shows that for different non-Gaussian parameters f_{NL} , current N_{eff} observations can effectively constrain the amplitude of the small-scale primordial power spectrum A_ζ . For the abundance of primordial black holes, the current N_{eff} observations can only effectively limit the abundance of primordial black holes with a mass around $m_{\text{pbh}} = 10^{-12} M_\odot$ when the non-Gaussian parameter f_{pbh} is less than zero and within a narrow range near

zero. For $f_{\text{NL}} > 0$ values, the $f_{\text{pbh}} = 1$ curves fall entirely within the allowable range of current N_{eff} observations.

To more clearly demonstrate the effect of third-order SIGWs on current N_{eff} observations, we provide a comparative illustration of the upper limits of A_ζ based on N_{eff} observational data, with and without the influence of third-order SIGWs. As shown in Fig. 3, the solid blue line represents the upper limit of A_ζ when third-order SIGWs are considered. The dashed green line represents the upper limit of A_ζ when the two-point correlation functions $\langle h_{\mathbf{k}}^{\lambda,(3)} h_{\mathbf{k}'}^{\lambda',(2)} \rangle$ and $\langle h_{\mathbf{k}}^{\lambda,(3)} h_{\mathbf{k}'}^{\lambda',(3)} \rangle$ are neglected. Our results indicate that for small absolute values of f_{NL} , third-order SIGWs greatly reduce the upper limit of A_ζ . For larger absolute values of f_{NL} , the non-Gaussian contribution from second-order SIGWs becomes dominant, and the influence of third-order SIGWs on the total energy density is comparatively minor. As the absolute value of f_{NL} increases, the blue solid line and the green dashed line in Fig. 3 gradually coincide. Furthermore, unlike the scenario considering only second-order SIGWs, due to the presence of the cross-correlation function $\langle h_{\mathbf{k}}^{\lambda,(3)} h_{\mathbf{k}'}^{\lambda',(2)} \rangle \sim f_{\text{NL}} A_\zeta^3$, the blue solid line in Fig. 3 is not symmetric about $f_{\text{NL}} = 0$.

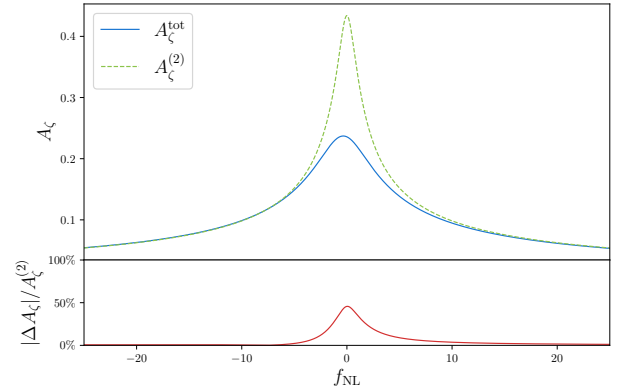


Figure 3. Constraints on A_ζ under different values of f_{NL} . Symbol $A_\zeta^{(2)}$ denotes the upper limit for A_ζ determined from N_{eff} observations, taking into account only the second-order SIGWs. Symbol A_ζ^{tot} denotes the upper limit for A_ζ determined from N_{eff} observations, considering all two-point correlation functions in Eq. (15). $\Delta A_\zeta = A_\zeta^{(2)} - A_\zeta^{\text{tot}}$ denotes the difference between the two upper bounds of A_ζ .

5. CONCLUSION AND DISCUSSION

We investigated the impact of SIGWs as an additional radiation component on cosmological evolution. By utilizing the parameter N_{eff} from current large-scale cosmological observations, we can place stringent limits on

the energy density of these waves. This allows us to constrain the parameter space of the small-scale primordial power spectrum and PBHs. In this paper, we calculated the total energy density of SIGWs up to A_ζ^3 order, taking into account a non-Gaussian primordial power spectrum. Our results indicate that the parameter space of the primordial power spectrum can be significantly constrained. Additionally, the current N_{eff} observations can effectively constrain the primordial black hole abundance only if the non-Gaussian parameter f_{NL} is less than zero and within a narrow range near zero. For $f_{\text{NL}} > 0$, the current N_{eff} observations cannot effectively constrain the abundance of PBHs.

To more effectively limit the parameter space of the small-scale primordial power spectrum and PBHs, future more precise N_{eff} observational data can be considered. A decrease in ΔN_{eff} will inevitably result in a reduced parameter space for the primordial power spectrum and PBHs. Furthermore, the influence of additional radiation components, apart from SIGWs, can also be taken into account Ghoshal et al. (2023); Roy Choudhury et al. (2022); Gerbino et al. (2023); Luo et al. (2020); Escudero Abenza (2020); Bennett et al. (2020). In this scenario, SIGWs and other extra radiation components will collectively impact the N_{eff} parameter. Current N_{eff} observational data can be utilized to constrain the parameter space of multiple extra radia-

tion components simultaneously. These topics may be explored in future research.

In this paper, we consider the contributions of the lowest-order non-Gaussian primordial perturbations to the total energy density spectrum of SIGWs. When fully accounting for non-Gaussian primordial perturbations, an additional term should be included in Eq. (15) Perna et al. (2024); Chang et al. (2024b): $\langle h_{\mathbf{k}}^{\lambda,(3)} h_{\mathbf{k}'}^{\lambda',(2)} \rangle \sim f_{\text{NL}} A_\zeta^3 + (f_{\text{NL}})^3 A_\zeta^4 + (f_{\text{NL}})^5 A_\zeta^5$ and $\langle h_{\mathbf{k}}^{\lambda,(2)} h_{\mathbf{k}'}^{\lambda',(2)} \rangle \sim (f_{\text{NL}})^2 A_\zeta^3 + (f_{\text{NL}})^4 A_\zeta^4$. Furthermore, here we only consider the contributions of SIGWs up to the third order. When the amplitude A_ζ of the small-scale primordial power spectrum is very large, the contributions of higher-order SIGWs cannot be ignored Zhou et al. (2024b). These contributions of higher-order non-Gaussianity and higher-order SIGWs will significantly enhance the energy density spectrum of SIGWs, thereby making the constraints of N_{eff} on the primordial power spectrum and the parameter space of PBHs more stringent. In this study, we investigated the contributions to the energy density spectrum of SIGWs up to the A_ζ^3 order. The resulting constraints can still be used as an upper limit for the abundance of PBHs. Future research may further refine the study of higher-order contributions.

The work is supported in part by the National Natural Science Foundation of China (NSFC) grants No.12475075, No.11935009, No.12375052, No.12075249, No.11690022, No.12275276, and No.12447127.

REFERENCES

- Abdalla, E., et al. 2022, JHEAp, 34, 49,
doi: [10.1016/j.jheap.2022.04.002](https://doi.org/10.1016/j.jheap.2022.04.002)
- Adshead, P., Lozanov, K. D., & Weiner, Z. J. 2021, JCAP, 10, 080, doi: [10.1088/1475-7516/2021/10/080](https://doi.org/10.1088/1475-7516/2021/10/080)
- Agazie, G., et al. 2023, Astrophys. J. Lett., 951, L8,
doi: [10.3847/2041-8213/acdac6](https://doi.org/10.3847/2041-8213/acdac6)
- Aghanim, N., et al. 2020, Astron. Astrophys., 641, A6,
doi: [10.1051/0004-6361/201833910](https://doi.org/10.1051/0004-6361/201833910)
- Ananda, K. N., Clarkson, C., & Wands, D. 2007, Phys. Rev. D, 75, 123518, doi: [10.1103/PhysRevD.75.123518](https://doi.org/10.1103/PhysRevD.75.123518)
- Antoniadis, J., et al. 2023, Astron. Astrophys., 678, A50,
doi: [10.1051/0004-6361/202346844](https://doi.org/10.1051/0004-6361/202346844)
- Barack, L., et al. 2019, Class. Quant. Grav., 36, 143001,
doi: [10.1088/1361-6382/ab0587](https://doi.org/10.1088/1361-6382/ab0587)
- Baumann, D., Steinhardt, P. J., Takahashi, K., & Ichiki, K. 2007, Phys. Rev. D, 76, 084019,
doi: [10.1103/PhysRevD.76.084019](https://doi.org/10.1103/PhysRevD.76.084019)
- Ben-Dayan, I., Keating, B., Leon, D., & Wolfson, I. 2019, JCAP, 06, 007, doi: [10.1088/1475-7516/2019/06/007](https://doi.org/10.1088/1475-7516/2019/06/007)
- Bennett, J. J., Buldgen, G., Drewes, M., & Wong, Y. Y. Y. 2020, JCAP, 03, 003,
doi: [10.1088/1475-7516/2020/03/003](https://doi.org/10.1088/1475-7516/2020/03/003)
- Bird, S., Cholis, I., Muñoz, J. B., et al. 2016, Phys. Rev. Lett., 116, 201301, doi: [10.1103/PhysRevLett.116.201301](https://doi.org/10.1103/PhysRevLett.116.201301)
- Bringmann, T., Scott, P., & Akrami, Y. 2012, Phys. Rev. D, 85, 125027, doi: [10.1103/PhysRevD.85.125027](https://doi.org/10.1103/PhysRevD.85.125027)
- Bugaev, E., & Klimai, P. 2010, Phys. Rev. D, 81, 023517,
doi: [10.1103/PhysRevD.81.023517](https://doi.org/10.1103/PhysRevD.81.023517)
- . 2011, Phys. Rev. D, 83, 083521,
doi: [10.1103/PhysRevD.83.083521](https://doi.org/10.1103/PhysRevD.83.083521)
- Byrnes, C. T., Cole, P. S., & Patil, S. P. 2019, JCAP, 06, 028, doi: [10.1088/1475-7516/2019/06/028](https://doi.org/10.1088/1475-7516/2019/06/028)
- Byrnes, C. T., Copeland, E. J., & Green, A. M. 2012, Phys. Rev. D, 86, 043512, doi: [10.1103/PhysRevD.86.043512](https://doi.org/10.1103/PhysRevD.86.043512)

- Cai, R.-g., Pi, S., & Sasaki, M. 2019, Phys. Rev. Lett., 122, 201101, doi: [10.1103/PhysRevLett.122.201101](https://doi.org/10.1103/PhysRevLett.122.201101)
- Cang, J., Ma, Y.-Z., & Gao, Y. 2023, Astrophys. J., 949, 64, doi: [10.3847/1538-4357/acc949](https://doi.org/10.3847/1538-4357/acc949)
- Carr, B., Kohri, K., Sendouda, Y., & Yokoyama, J. 2021, Rept. Prog. Phys., 84, 116902, doi: [10.1088/1361-6633/ac1e31](https://doi.org/10.1088/1361-6633/ac1e31)
- Chang, Z., Kuang, Y.-T., Wu, D., & Zhou, J.-Z. 2024a, JCAP, 2024, 044, doi: [10.1088/1475-7516/2024/04/044](https://doi.org/10.1088/1475-7516/2024/04/044)
- Chang, Z., Kuang, Y.-T., Wu, D., Zhou, J.-Z., & Zhu, Q.-H. 2024b, Phys. Rev. D, 109, L041303, doi: [10.1103/PhysRevD.109.L041303](https://doi.org/10.1103/PhysRevD.109.L041303)
- Chang, Z., Kuang, Y.-T., Zhang, X., & Zhou, J.-Z. 2023, Chin. Phys. C, 47, 055104, doi: [10.1088/1674-1137/acc649](https://doi.org/10.1088/1674-1137/acc649)
- Chen, C., Ghoshal, A., Tasinato, G., & Tomberg, E. 2024, <https://arxiv.org/abs/2409.12950>
- Chen, C., Ota, A., Zhu, H.-Y., & Zhu, Y. 2023, Phys. Rev. D, 107, 083518, doi: [10.1103/PhysRevD.107.083518](https://doi.org/10.1103/PhysRevD.107.083518)
- Choudhury, S., Ganguly, S., Panda, S., SenGupta, S., & Tiwari, P. 2024, JCAP, 09, 013, doi: [10.1088/1475-7516/2024/09/013](https://doi.org/10.1088/1475-7516/2024/09/013)
- Clarke, T. J., Copeland, E. J., & Moss, A. 2020, JCAP, 10, 002, doi: [10.1088/1475-7516/2020/10/002](https://doi.org/10.1088/1475-7516/2020/10/002)
- Domènech, G. 2021, Universe, 7, 398, doi: [10.3390/universe7110398](https://doi.org/10.3390/universe7110398)
- Domènech, G., Pi, S., Wang, A., & Wang, J. 2024, JCAP, 08, 054, doi: [10.1088/1475-7516/2024/08/054](https://doi.org/10.1088/1475-7516/2024/08/054)
- Domènech, G., & Tränkle, J. 2024, <https://arxiv.org/abs/2409.12125>
- Ellis, J., Fairbairn, M., Franciolini, G., et al. 2024, Phys. Rev. D, 109, 023522, doi: [10.1103/PhysRevD.109.023522](https://doi.org/10.1103/PhysRevD.109.023522)
- Escudero Abenza, M. 2020, JCAP, 05, 048, doi: [10.1088/1475-7516/2020/05/048](https://doi.org/10.1088/1475-7516/2020/05/048)
- Franciolini, G., Iovino, Junior., A., Vaskonen, V., & Veermae, H. 2023, Phys. Rev. Lett., 131, 201401, doi: [10.1103/PhysRevLett.131.201401](https://doi.org/10.1103/PhysRevLett.131.201401)
- García-Bellido, J. 2017, J. Phys. Conf. Ser., 840, 012032, doi: [10.1088/1742-6596/840/1/012032](https://doi.org/10.1088/1742-6596/840/1/012032)
- Gerbino, M., et al. 2023, Phys. Dark Univ., 42, 101333, doi: [10.1016/j.dark.2023.101333](https://doi.org/10.1016/j.dark.2023.101333)
- Ghoshal, A., Lalak, Z., & Porey, S. 2023, Phys. Rev. D, 108, 063030, doi: [10.1103/PhysRevD.108.063030](https://doi.org/10.1103/PhysRevD.108.063030)
- Harada, T., Yoo, C.-M., & Kohri, K. 2013, Phys. Rev. D, 88, 084051, doi: [10.1103/PhysRevD.88.084051](https://doi.org/10.1103/PhysRevD.88.084051)
- Harigaya, K., Inomata, K., & Terada, T. 2023, Phys. Rev. D, 108, 123538, doi: [10.1103/PhysRevD.108.123538](https://doi.org/10.1103/PhysRevD.108.123538)
- Hosseini Mansoori, S. A., Felegray, F., Talebian, A., & Sami, M. 2023, JCAP, 08, 067, doi: [10.1088/1475-7516/2023/08/067](https://doi.org/10.1088/1475-7516/2023/08/067)
- Jiang, J.-Q., Cai, Y., Ye, G., & Piao, Y.-S. 2024, JCAP, 05, 004, doi: [10.1088/1475-7516/2024/05/004](https://doi.org/10.1088/1475-7516/2024/05/004)
- Kohri, K., & Terada, T. 2018, Phys. Rev. D, 97, 123532, doi: [10.1103/PhysRevD.97.123532](https://doi.org/10.1103/PhysRevD.97.123532)
- Luo, X., Rodejohann, W., & Xu, X.-J. 2020, JCAP, 06, 058, doi: [10.1088/1475-7516/2020/06/058](https://doi.org/10.1088/1475-7516/2020/06/058)
- Matarrese, S., Mollerach, S., & Bruni, M. 1998, Phys. Rev. D, 58, 043504, doi: [10.1103/PhysRevD.58.043504](https://doi.org/10.1103/PhysRevD.58.043504)
- Mollerach, S., Harari, D., & Matarrese, S. 2004, Phys. Rev. D, 69, 063002, doi: [10.1103/PhysRevD.69.063002](https://doi.org/10.1103/PhysRevD.69.063002)
- Musco, I., Miller, J. C., & Polnarev, A. G. 2009, Class. Quant. Grav., 26, 235001, doi: [10.1088/0264-9381/26/23/235001](https://doi.org/10.1088/0264-9381/26/23/235001)
- Musco, I., Miller, J. C., & Rezzolla, L. 2005, Class. Quant. Grav., 22, 1405, doi: [10.1088/0264-9381/22/7/013](https://doi.org/10.1088/0264-9381/22/7/013)
- Papanikolaou, T. 2023, PoS, CORFU2022, 265, doi: [10.22323/1.436.0265](https://doi.org/10.22323/1.436.0265)
- Papanikolaou, T., Banerjee, S., Cai, Y.-F., Capozziello, S., & Saridakis, E. N. 2024, JCAP, 06, 066, doi: [10.1088/1475-7516/2024/06/066](https://doi.org/10.1088/1475-7516/2024/06/066)
- Papanikolaou, T., Vennin, V., & Langlois, D. 2021, JCAP, 03, 053, doi: [10.1088/1475-7516/2021/03/053](https://doi.org/10.1088/1475-7516/2021/03/053)
- Perna, G., Testini, C., Ricciardone, A., & Matarrese, S. 2024, JCAP, 05, 086, doi: [10.1088/1475-7516/2024/05/086](https://doi.org/10.1088/1475-7516/2024/05/086)
- Reardon, D. J., et al. 2023, Astrophys. J. Lett., 951, L6, doi: [10.3847/2041-8213/acdd02](https://doi.org/10.3847/2041-8213/acdd02)
- Roy Choudhury, S., Hannestad, S., & Tram, T. 2022, JCAP, 10, 018, doi: [10.1088/1475-7516/2022/10/018](https://doi.org/10.1088/1475-7516/2022/10/018)
- Saikawa, K., & Shirai, S. 2018, JCAP, 05, 035, doi: [10.1088/1475-7516/2018/05/035](https://doi.org/10.1088/1475-7516/2018/05/035)
- Saito, R., & Yokoyama, J. 2009, Phys. Rev. Lett., 102, 161101, doi: [10.1103/PhysRevLett.102.161101](https://doi.org/10.1103/PhysRevLett.102.161101)
- Sasaki, M., Suyama, T., Tanaka, T., & Yokoyama, S. 2018, Class. Quant. Grav., 35, 063001, doi: [10.1088/1361-6382/aaa7b4](https://doi.org/10.1088/1361-6382/aaa7b4)
- Sui, X.-B., Liu, J., Yang, X.-Y., & Cai, R.-G. 2024, <https://arxiv.org/abs/2407.04220>
- Wang, S., Terada, T., & Kohri, K. 2019, Phys. Rev. D, 99, 103531, doi: [10.1103/PhysRevD.99.103531](https://doi.org/10.1103/PhysRevD.99.103531)
- Wang, S., Zhao, Z.-C., & Zhu, Q.-H. 2024, Phys. Rev. Res., 6, 013207, doi: [10.1103/PhysRevResearch.6.013207](https://doi.org/10.1103/PhysRevResearch.6.013207)
- Wright, D., Giblin, J. T., & Hazboun, J. 2024, <https://arxiv.org/abs/2409.15572>
- Xu, H., et al. 2023, Res. Astron. Astrophys., 23, 075024, doi: [10.1088/1674-4527/acdfa5](https://doi.org/10.1088/1674-4527/acdfa5)
- Young, S., & Byrnes, C. T. 2013, JCAP, 08, 052, doi: [10.1088/1475-7516/2013/08/052](https://doi.org/10.1088/1475-7516/2013/08/052)
- Yu, Y.-H., & Wang, S. 2024, <https://arxiv.org/abs/2405.02960>

- Yuan, C., Chen, Z.-C., & Huang, Q.-G. 2019, Phys. Rev. D, 100, 081301, doi: [10.1103/PhysRevD.100.081301](https://doi.org/10.1103/PhysRevD.100.081301)
- Zhou, J.-Z., Kuang, Y.-T., Wu, D., et al. 2024a.
<https://arxiv.org/abs/2409.07702>
- Zhou, J.-Z., Kuang, Y.-T., Wu, D., Lü, H., & Chang, Z. 2024b. <https://arxiv.org/abs/2408.14052>
- Zhou, J.-Z., Zhang, X., Zhu, Q.-H., & Chang, Z. 2022, JCAP, 05, 013, doi: [10.1088/1475-7516/2022/05/013](https://doi.org/10.1088/1475-7516/2022/05/013)